Kämpf, L., Brauer, A., Swierczynski, T., Czymzik, M., Müller, P., Dulski, P. (2014): Processes of flood-triggered detrital layer deposition in the varved Lake Mondsee sediment record revealed by a dual calibration approach. - *Journal of Quaternary Science*, *29*, 5, p. 475-486

DOI: http://doi.org/10.1002/jqs.2721

Processes of flood-triggered detrital layer deposition in the varved Lake Mondsee sediment record revealed by a dual calibration approach

Lucas Kämpf, Achim Brauer, Tina Swierczynski, Markus Czymzik, Philip Mueller, Peter Dulski

Helmholtz-Centre Potsdam – German Research Centre for Geosciences (GFZ), Telegrafenberg, 14473 Potsdam, Germany

Abstract A succession of 23 sub-millimetre to maximum 12 mm thick, mostly flood-triggered detrital layers, deposited between 1976 and 2005, was analysed in 12 varved surface sediment cores from meso-scale peri-alpine Lake Mondsee applying microfacies and high-resolution micro-XRF analyses. Detailed intra-basin comparison of these layers enabled identification of (i) different source areas of detrital sediments, (ii) flood-triggered sediment flux and local erosion events, and (iii) seasonal differences of suspended flood sediment distribution within the lake basin.

Additional calibration of the detrital layer record with river discharge and precipitation data reveals different empirical thresholds for flood layer deposition for different parts of the basin. At proximal locations detrital layer deposition requires floods exceeding a daily discharge of 40 m^3s^{-1}, whereas at a 2 km more distal location an hourly discharge of 80 m^3s^{-1} and at least 2 days of discharge above 40 m^3s^{-1} is necessary. Furthermore, we observe a better correlation between layer thickness and flood amplitude in the depocentre than in distal and proximal areas of the basin. Although our results are partly site-specific, the applied dual calibration approach is suitable to precisely decipher flood layer formation processes and, thereby, improve the interpretation of long flood time series from lake sediments.

1 Introduction

Detrital layers in lake sediments are valuable recorders of extreme river floods (Siegenthaler and Sturm, 1991; Chapron *et al.*, 2005; Gilli *et al.*, 2013) and thus increasingly used to establish continuous long flood chronologies reaching several millennia back in time (Arnaud *et al.*, 2005; Lauterbach *et al.*, 2012; Czymzik *et al.*, 2013; Swierczynski *et al.*, 2013). The recurrence intervals of detrital layers provides information about palaeoflood frequencies (Czymzik *et al.*, 2010; Glur *et al.*, 2013), whereas flood intensities have been inferred from the thickness of individual deposits (Desloges and Gilbert, 1994; Brown *et al.*, 2000; Wilhelm *et al.*, 2013). Varved sediment records provide the unique opportunity to date detrital layers with seasonal precision (Mangili *et al.*, 2005) and, thereby, determine palaeoflood variability even at seasonal scale (Lamoureux, 2000; Czymzik *et al.*, 2010; Swierczynski *et al.*, 2012; Wirth *et al.*, 2013).

Despite the great potential especially of varved lake sediments for reconstructing long flood time series, there are still some confinements in interpreting detrital layer records due to a lack in understanding the complex chain of processes from an extreme rainfall event to the deposition of a fine layer of eroded catchment material on the lake floor. One important issue under discussion is the completeness of detrital layer flood time series. Detailed comparisons with instrumental hydrological data have revealed that detrital layer records can be biased by individual layers triggered by local erosion events rather than by floods (Kämpf *et al.*, 2012b; Swierczynski *et al.*, 2012; Simonneau *et al.*, 2013) and by individual flood events that are not recorded in the sediments (Lamoureux, 2000; Gilli *et al.*, 2003; Swierczynski *et al.*, 2009; Czymzik *et al.*, 2010; Schiefer *et al.*, 2011). Moreover, there is a lack of knowledge about the internal distribution of detrital sediments within lake basins, which, however, is important to determine the best coring location for flood reconstruction.

To better decipher processes of detrital flood layer deposition in lake sediments, several approaches have been initiated including in situ monitoring of flood triggered sediment fluxes (Cockburn and Lamoureux, 2008; Crookshanks and Gilbert, 2008) and detailed comparisons of single flood deposits with instrumental flood data (Gilbert *et al.*, 2006; Schiefer *et al.*, 2006; Kämpf *et al.*, 2012a). Here we present a new dual calibration approach for the detrital layer record from varved sediments of Lake Mondsee (Upper Austria) covering the Mid- to Late Holocene (Swierczynski *et al.*, 2013). This approach integrates (i) precise intra-basin correlation of detrital layers along transects from three near delta locations to a deep water distal site applying microscopic techniques, and, (ii) event-based calibration of detrital flood layers with precipitation and river discharge data over a 30-year period. The main goal of this study is to investigate the relations between hydrological conditions and detrital layer deposition and therewith to evaluate: (i) threshold values for detrital layer deposition, (ii) the completeness of flood layer records in dependence from their location within the lake basin and

(iii) the causes for flood events not leading to detrital layer deposition. Therewith we aim at an improved understanding of detrital layer deposition in Lake Mondsee and reconstruction of past flood variability with general relevance also for flood reconstructions from other lacustrine sediment records.

2 Study site

Lake Mondsee is located at the northern fringe of the European Alps in Upper Austria (47°48'N, 13°23'E) at an altitude of 481 m above sea level (a.s.l.). With a surface of 14 km^2 the lake represents a meso-scale peri-alpine lake which is by a factor of 2-3 smaller than the previously studied peri-alpine lakes Brienz, Bourget and Ammersee and even by a factor of 40 smaller than the largest peri-alpine lakes Geneva and Constance. Lake Mondsee has a maximum water depth of 68 m and is a meromictic hardwater lake with one mixing period in autumn/winter. A thermal stratification of the lake water column is established from May to September (Dokulil and Skolaut, 1986). Lake Mondsee has a specific shape which is different from other peri-alpine lakes and displays a significant kink in the generally elongated and NW-SE directed shape (Fig. 4.1c). In addition, the main tributary and source for suspended sediments, the Griesler Ache, flows into the lake from the West at the kink position where the lake basin is N-S directed so that the continuation of the water flow in the lake is not, as in the other peri-alpine lakes, directed straight to the outflow but makes a 90° turn.

The catchment (247 km^2) is subdivided into two major geological units by a main alpine thrust fault (van Husen, 1989) following the southern shoreline of the lake (Fig.1b). The northern catchment (ca. 75% of the total catchment) is formed by smooth peri-alpine hills of up to 1100 m a.s.l. which are built up by Cretaceous Flysch sediments (Sandstone, Argillite). The valleys are covered by moraines formed by latest Pleistocene glacier activity (van Husen, 1989). Three tributaries drain the northern catchment: the main inflow Griesler Ache in the West draining an area of 109 km^2 and forming a distinct delta as well as Zeller Ache in the North and Wangauer Ache in the East. The southern sub-catchment (ca. 25%) reaches a maximum elevation of 1700 m a.s.l. and belongs to the Northern Calcareous Alps. The base rock is composed of Jurassic and Triassic units of limestone and dolomite forming steep slopes at the southern lake shoreline which are drained by small torrents, e.g. the Kienbach creek with a catchment of 2.1 km^2 (Fig. 4.1c). The outflow of Lake Mondsee is located at the south-eastern end of the lake and drains the lake via the river Seeache into Lake Attersee (Fig. 4.1c).

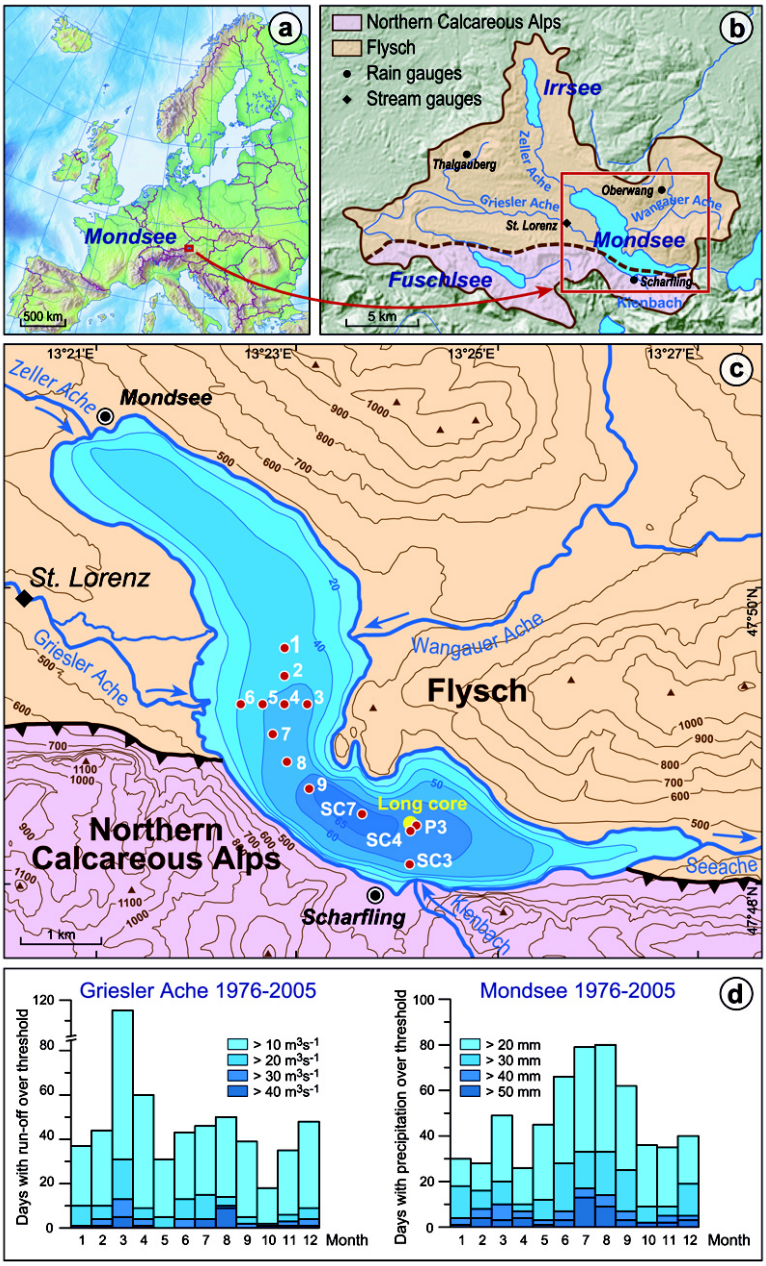

Figure 1. Lake Mondsee study site and climatic situation: (a) location, (b) Lake Mondsee catchment: dots indicate rain gauges and the stream gauge at Griesler Ache, (c) Bathymetric map of Lake Mondsee: dots indicate short cores retrieved in 2010 (1-9), 2007 (SC3-7), 2005 (P3 + long core profile), Fig. 4.1 a-c modified after Lauterbach *et al.* (2011), (d) monthly distribution of runoff events (left, Griesler Ache) and precipitation events (right, Mondsee).

The mean annual air temperature at climate station of Mondsee (reference period 1971-2000) is 8.7 °C with temperatures of -0.5 °C and +17.5 °C in January and July, respectively. The mean annual precipitation is 1550 mm and shows maxima during summer (Fig. 4.1d). Accordingly, floods mainly occur in summer and subordinated in early spring and rarely in winter. In summer, floods are triggered by short-term intense precipitation. The typical circulation pattern, reasonable for ca. 70% of the most extreme summer floods, is a low pressure cell or trough over Central to Western Europe (Tab. 4.2) generating a flow of very moist air from the Mediterranean Sea (Parajka *et al.*, 2010). This weather type is known as “Vb”-

type (Petrow *et al.*, 2009), and triggers the most extreme floods in Central Europe (Mudelsee *et al.*, 2004; Petrow *et al.*, 2009). The remaining events (ca. 30%) are related to northerly and westerly storm tracks (Tab. 4.2). Strong spring and winter floods are caused by precipitation events and associated rapid melting of snow. Frontal rainfall in that time is usually triggered by westerly circulation patterns (Tab. 4.2) carrying warm and moist air masses from the Atlantic Ocean (Petrow *et al.*, 2009; Parajka *et al.*, 2010).

3 Methods

13 short cores were recovered from Lake Mondsee (Fig. 4.1c) during three coring campaigns (2005, 2007, 2010) using a UWITEC Gravity Corer (60 and 90 mm in diameter). These cores are 72 to 160 cm long and have been collected in water depths between 34 m and 65 m (Tab. 4.4) following three transects along the steepest slope gradients in order to distinguish sediment source areas: (i) from the main inflow, Griesler Ache, to the long master core sequence used for establishing a long flood layer record (Swierczynski *et al.*, 2013); (ii) between the main (Griesler Ache) and the secondary (Wangauer Ache) tributary; (iii) from the Kienbach creek inflow draining the steep southern catchment into the southern part of the lake basin close to the location of the master core.

After cutting the sediment cores into two halves, lithological description and digital photographs on the split core surface were carried out. Overlapping samples for large-format (10 cm x 2 cm) thin sections for micro-facies analyses were taken from the fresh sediment surface. Thin sections were prepared according to the method described by Brauer and Casanova (2001). Microfacies analyses have been carried out under plain and polarized light conditions and magnifications between 20x and 400x, using a petrographic microscope (Olympus BX53). Thin-section images were obtained with a digital camera (Olympus DP72) and the software Olympus CellSens Dimension.

Micro- X-ray fluorescence (µ-XRF) scanning has been conducted to the upper 26 cm of cores MO/10/1, 4, 5, 7, 8, 9, MO/07/SC3 and MO/05/P3 using an EAGLE III XL µ-XRF spectrometer with a low power Rh X-ray tube at 40 kV and 300 µA. All measurements were performed under vacuum on a single scan line with 250 µm spot size, 200 µm step width and a counting time of 60 s. Each data point reflects the mean element intensity, expressed in counts per second (cps). Micro-facies data were interpreted in combination with element data obtained by µ-XRF scanning on those impregnated sediment slabs from which thin sections have been prepared. This allowed direct comparison of geochemical and micro-facies data (Brauer *et al.*, 2009).

The chronology of the sediment cores was established by varve counting, intra-basin correlation to the master core MO/05/P3, dated by varve counting and

additional ^{137}Cs measurements (Swierczynski *et al.*, 2009), as well as the identification of two marker diatom layers dated to 1983 and 1986 (Klee and Schmidt, 1987; Schmidt, 1991).

The sediment record was compared with regional flood data. Discharge in the main tributary, Griesler Ache, is recorded by the hydrographic service of Upper Austria at the St. Lorenz gauging station (Fig. 4.1b). Precipitation data are obtained from the rain gauges in Thalgauberg (Griesler Ache), supplied by the hydrographic service of Land Salzburg, Oberwang (Wangauer Ache) and Scharfling (Kienbach), measured by the hydrographic service of Upper Austria (Fig. 4.1b). We used hourly and daily data for the period 1976-2005 covered by hydrological and sedimentological datasets.

4 Results

4.1 Sedimentology

Mid- to Late Holocene sediments from Lake Mondsee sediments are formed by biochemical calcite varves comprising light and dark sub-layers (Lauterbach *et al.*, 2011). Light sub-layers are composed of fine calcite crystals (< 5 µm) clearly reflected in µ-XRF calcium peaks (Fig. 4.2). Dark sub-layers consist of clay to silt sized mixed organic-minerogenic material indicated by secondary peaks in titanium used as a proxy for detrital input from the northern Flysch catchment (Swierczynski *et al.*, 2012). Correlation coefficients of $r^2 = 0.70 - 0.75$ to aluminium, potassium and silica confirm the predominately detrital origin of all these elements. Sediment cores in the deep southern basin (MO/05/P3: 62 m, MO/07/SC4: 64 m water depth) are entirely varved. However, varve preservation in sediment sequences retrieved from shallower coring sites (< 60 m) is limited to the uppermost decimetres leading to a broad lithological division into a homogeneous lower sediment unit I and a varved sediment unit II (Fig. 4.2). The transition between both units is gradual and occurs between 18 cm sediment depth in the central basin (MO/10/9) and 37 cm proximal to the river inflow (MO/10/5) (Tab. S.1). The lamination in sediment unit I appears indistinct in the proximal basin (MO/10/5: 47 m) and is absent in sediment cores from shallower parts of the lake (MO/10/6: 34 m).

Sediment unit II was further divided into three sub-units based on sediment colour and varve micro-facies (Swierczynski *et al.*, 2009). Our investigation on detrital layers is confined to the uppermost part of sediment unit II (Fig. 4.2), ranging in thickness from 5.5 cm in the distal core MO/05/P3 to 16 cm in the proximal core MO/10/5 and containing 28 (MO/05/P3) to 33 (MO/10 cores) distinct varves. The only non-varved sediment core from the shallow delta area (MO/10/6) was not considered for further investigations.

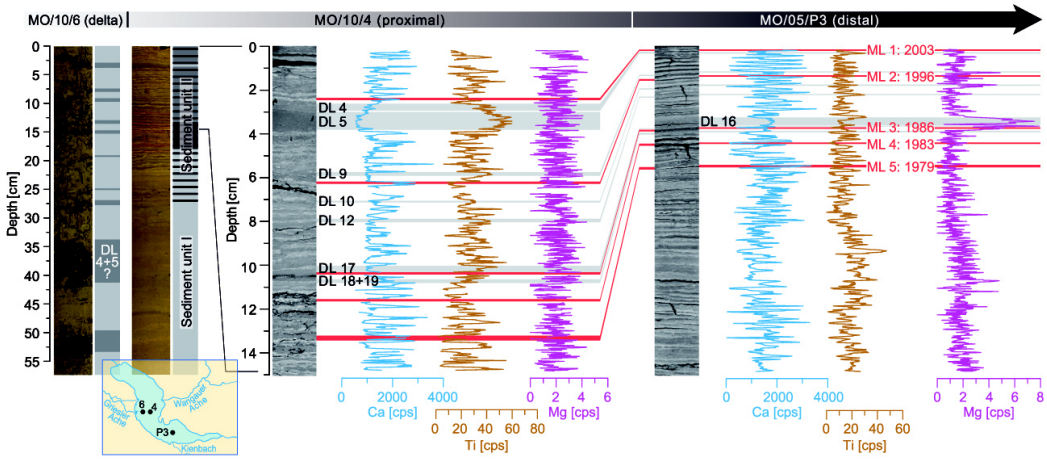

Figure 2. Lithology of Lake Mondsee sediments: MO/10/6 (310 m to the main inflow Griesler Ache/ 34 m water depth), MO/10/4 (820 m/ 55 m), MO/05/P3 (2850 m/ 62 m). Sediment unit II is shown in detail for cores MO/10/4 and MO/05/P3 by thin section scans and µ-XRF profiles of calcium (Ca) as proxy for endogenic calcite precipitation, titanium (Ti) as proxy for detrital input from the Flysch zone and magnesium (Mg) as proxy for detrital input from the Northern Calcareous Alps. Red bars indicate marker layers for core-to-core correlation (ML 1-5); grey bars indicate correlated detrital layers (DL).

4.2 Chronology

In order to establish precise calendar year chronologies for each sediment core, varve counting in thin sections has been independently carried out for each individual core sequence. Intra-basin correlation has been performed by using three distinct calcite layers (ML 1: 2003, ML 2: 1996, ML 5: 1979) and two diatom layers (ML 3: 1986, ML 4: 1983) marking well-documented shifts in diatom composition (Klee and Schmidt, 1987; Schmidt, 1991). Based on these markers all sediment cores have been correlated to the master core sequence MO/05/P3 indicating the top of the long sediment record (Lauterbach *et al.*, 2011; Swierczynski *et al.*, 2012). Varve counting is in agreement with ^{137}Cs peaks in core MO/05/P3 (Lauterbach *et al.*, 2011; Swierczynski *et al.*, 2012).

Varve formation (sediment unit II) in most of the Lake Mondsee sediment cores commences between 1953 and 1957 (Tab. 4.4) allowing determining the season of deposition of detrital layers by their micro-stratigraphic position within single varves (Fig. 4.4). Summer detrital layers are deposited within or directly on top of calcite layers. Detrital layers deposited within the mixed layer are formed in autumn to early spring and are labelled as winter detrital layers. This allows allocating 17 summer detrital layers and 10 winter detrital layers for the investigated time period between 1976 and 2005 (Fig. 4.3, Tab. 4.1).

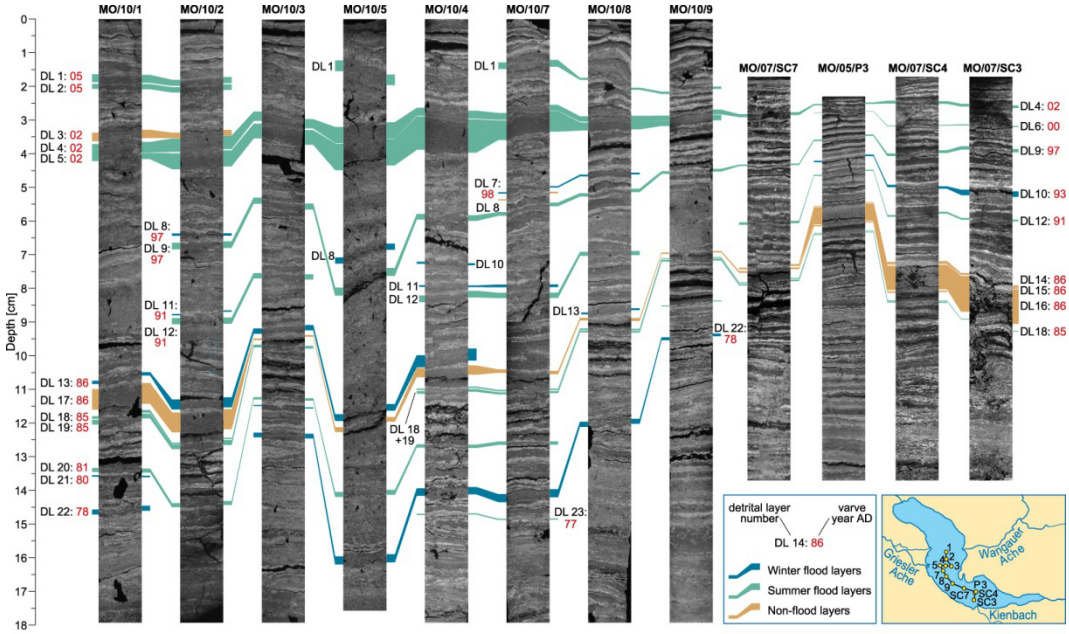

Figure 3. Intra-basin correlation of detrital layers in Lake Mondsee sediments (thin section scans) for the investigated period 1976-2005.

4.3 Detrital layer microfacies

27 detrital layers ranging in thickness from 0.1 to 12 mm have been detected in the investigated sediment cores labelled from top to down in the sediment sequences. Detrital layers can be clearly differentiated from calcite varves due to their composition of allochthonous minerogenic and, partly, organic matter originating from the catchment which is further reflected by distinct peaks in either titanium, a proxy for detrital matter from the northern Flysch catchment, or magnesium reflecting the southern catchment built up of limestone and dolomite or of both (Fig. 4.2).

Three main detrital microfacies have been distinguished (Tab. 4.1): (i) Graded layers (40% of all layers), (ii) silt/clay layers (30%) and (iii) matrix supported layers (30%). Graded layers range in thickness from 0.4-10 mm and are mainly composed of clastic material (quartz, feldspar, dolomite and calcite) and terrestrial plant debris. A typical feature in six graded layers is a normal upward fining (Fig. 4.4c+g). Four graded layers exhibit a more complex texture like an inversely graded basal bed overlain by a normal graded bed (layers DL 9, 12, 19; Fig. 4.4b+e) or a succession of two normal gradings (layer DL 4; Fig. 4.4g). Variations in maximum grain sizes observed in the basal layer part can be used to further distinguish between fine-grained (max. grain sizes < 10 µm; labelled with G-f in Tab. 4.1) and coarse grained layers (> 30 µm; G-c).

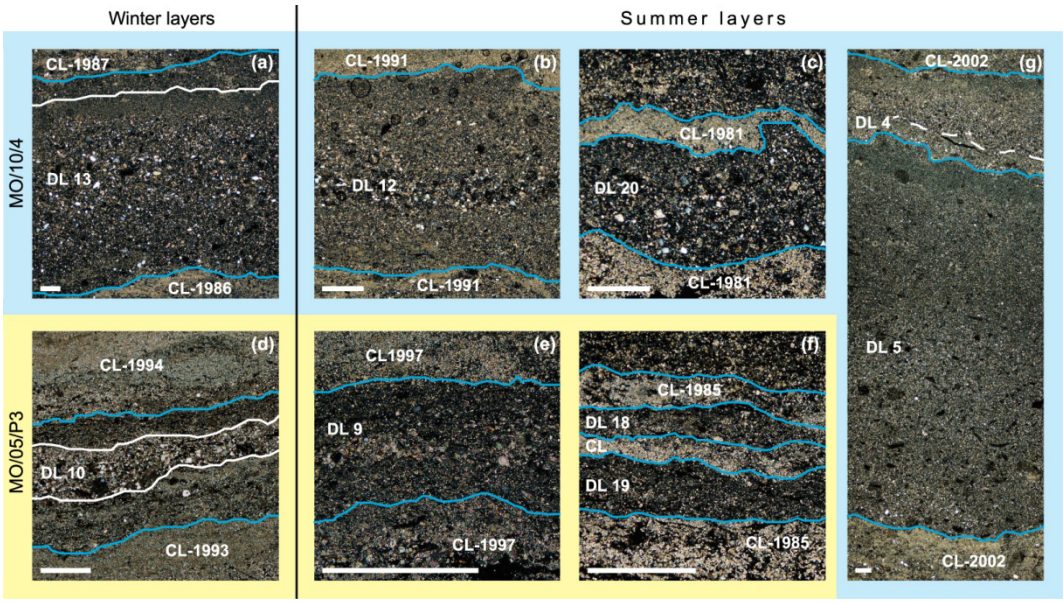

Figure 4. Detrital microfacies in the proximal core MO/10/4 (blue) and the distal master core MO/05/P3 (yellow): matrix supported layers: (a) DL 13, (d) DL 10; normally graded layers: (c) DL 20, (g) DL 5; two normally graded beds: (g) DL 4, separated by the dotted white line; inverse below normal grading: (b) DL 12, (e) DL 9; (f) Silt/clay layers: DL 18+19. White lines indicate detrital layer boundaries (DL + No.), blue lines indicate calcite layer boundaries (CL + varve year). White bars are equivalent to 0.4 mm.

Table 1. Detrital layers in the investigated uppermost part of Lake Mondsee sediments including layer thickness (in mm) and microfacies (MF).

Varve year + season	DL No.	MO 10/1		MO 10/2		MO 10/3		MO 10/5		MO 10/4		MO 10/7		MO 10/8		MO 10/9		MO 07/ SC7		MO 05/P3		MO 07/ SC4		MO 07/ SC3	
		[mm]	*MF*	[mm]	*MF*	[mm]	*MF*	[mm]	*MF*	[mm]	*MF*	[mm]	*MF*	[mm]	*MF*	[mm]	*MF*	[mm]	*MF*	[mm]	*MF*	[mm]	*MF*	[mm]	*MF*
2005 su	**1**	2.4	*M*	1.8	*M*	n. d.		3.2	*M*	-		2.0	*G-f*	0.6	*S*	0.7	*G-f*	0.4	*S*	-		n. d.		n. d.	
2005 su	**2**	1.5	*M*	1.6	*G*	n. d.		n. d.		-		n. d.		n. d.		n. d.		n. d.		-		n. d.		n. d.	
2002 wi	**3**	2.6	*M*	1.6	*M*	n. d.		n. d.		n. d.		n. d.		n. d.		n. d.		n. d.		n. d.		n. d.		n. d.	
2002 su	**4**	3.2	*G-c*	4.0	*G-c*	2.8	*G-c*	4.8	*G-c*	2.4	*G-c*	2.0	*G-c*	1.6	*G*	1.4	*G*	0.8	*G-f*	0.4	*S*	0.8	*G-f*	0.8	*G-f*
2002 su	**5**	1.8	*G-f*	4.8	*G-f*	4.4	*G-f*	8.0	*G-f*	10.0	*G-f*	6.5	*G-f*	2.4	*G-f*	1.6	*G-f*	n. d.		n. d.		n. d.		n. d.	
2000 su	**6**	n. d.		n. d.		n. d.		n. d.		n. d.		n. d.		n. d.		n. d.		n. d.		0.1	*M*	0.2	*M*	0.3	*M*
1998 wi	**7**	-		n. d.		n. d.		n. d.		-		0.4	*M*	0.5	*M*	n. d.		n. d.		n. d.		n. d.		n. d.	
1998 su	**DL**	-		n. d.		n. d.		n. d.		-		0.4		n. d.		n. d.		n. d.		n. d.		n. d.		n. d.	
1997 wi	**8**	-		0.7	*M*	n. d.		1.8	*M*	n. d.		0.6	*M*	n. d.		n. d.		n. d.		n. d.		n. d.		n. d.	
1997 su	**9**	-		2.0	*G-c*	1.8	*G-c*	2.4	*G-c*	1.7	*G-c*	1.1	*G-c*	1.0	*G-c*	0.8	*S*	0.4	*S*	0.4	*G*	0.8	*G*	1.0	*G*
1993 wi	**10**	-		n. d.		n. d.		-		0.6	*M*	n. d.		n. d.		-		n. d.		0.4	*M*	0.7	*M*	1.6	*M*
1991 wi	**11**	-		0.4	*M*	n. d.		-		0.5	*M*	0.8	*M*	n. d.		-		n. d.		n. d.		n. d.		n. d.	
1991 su	**12**	-		1.8	*G-c*	1.6	*G-f*	-		2.0	*G-c*	1.6	*G-c*	1.2	*G-c*	-		0.7	*S*	0.3	*S*	0.5	*S*	0.5	*G-f*
1990 wi	**DL**	-		3.5	*G-c*	n. d.		-		n. d.		n. d.		n. d.		-		n. d.		n. d.		n. d.		n. d.	
1989 wi	**DL**	-		0.6	*M*	n. d.		-		n. d.		n. d.		n. d.		-		n. d.		n. d.		n. d.		n. d.	
1986 wi	**13**	1.0	*M*	3.0	*M*	1.6	*M*	2.0	*M*	3.6	*G-c*	n. d.		0.6	*M*	-		n. d.		n. d.		n. d.		n. d.	
1986 su	**14**	n. d.		n. d.		n. d.		n. d.		n. d.		n. d.		n. d.		n. d.		n. d.		n. d.		0.5	*M*	0.4	*M*
1986 su	**15**	n. d.		n. d.		n. d.		n. d.		n. d.		n. d.		n. d.		n. d.		n. d.		0.2	*M*	0.2	*M*	0.5	*M*
1986 su	**16**	n. d.		n. d.		n. d.		n. d.		n. d.		n. d.		n. d.		n. d.		0.5	*G-c*	5.2	*M*	8.0	*M*	12.0	*M*
1986 su	**17**	6.2	*G-f*	6.0	*G-f*	0.5	*S*	0.5	*S*	2.8	*S*	1.0	*S*	0.8	*S*	0.4	*S*	0.5	*S*	0.3	*S*	0.4	*S*		
1985 su	**18**	0.8	*G-f*	0.4	*S*	n. d.		-		0.4	*S*	0.4	*S*	0.4	*S*	0.3	*S*	0.2	*S*	0.1	*S*	0.2	*S*	0.2	*S*
1985 su	**DL**	n. d.		n. d.		n. d.		-		n. d.		n. d.		n. d.		n. d.		n. d.		n. d.		n. d.		0.2	*M*
1985 su	**19**	1.4	*G-f*	1.4	*G-f*	0.8	*G-f*	-		0.8	*G-f*	0.6	*S*	0.5	*S*	0.5	*S*	0.4	*S*	0.2	*S*	0.3	*S*	n. d.	
1981 su	**20**	1.2	*G-f*	1.2	*M*	0.7	*G-f*	1.5	*M*	1.0	*G-c*	1.0	*G-c*	-		0.3	*S*	n. d.		n. d.		n. d.		0.5	*S*
1980 wi	**21**	0.5	*M*	n. d.		0.3	*S*	n. d.		n. d.		0.7	*M*	-		n. d.		n. d.		n. d.		n. d.		n. d.	
1978 wi	**22**	1.5	*G-c*	n. d.		1.4	*G-c*	2.4	*G-c*	2.2	*G-c*	2.4	*G-c*	1.5	*G-c*	0.8	*S*	n. d.		n. d.		n. d.		n. d.	
1977 su	**23**	-		-		n. d.		n. d.		0.4	*S*	0.4	*S*	-		-		n. d.		n. d.		n. d.		n. d.	

(M) Matrix supported layers, (S) silt-clay layers, (G) graded layers in combination with more specific microfacies features: very fine-grained (-f, max. grain size < 10 µm), very coarse-grained (-c, max. grain size > 30 µm). The absence of detrital layer deposition is indicated by the abbreviation n. d., dashes (-) point to disturbed sediment sequences or highly clastic background sedimentation and therefore possibly hidden detrital layers.

Silt/clay layers differ from graded layers mainly by the almost entirely minerogenic composition with grains rarely exceeding 10 µm in diameter and the lack of clear textural organization. The thickness of these layers varies between 0.1 and 6.2 mm. Some of the thinner (<0.5 mm) silt/clay layers appear as individual detrital grains aligned along the bedding (Fig. 4.4f) rather than as distinct layers.

Matrix supported layers range in thickness from 0.1 to 12 mm and contain minerogenic matter sizing between 30 and, partly, > 100 µm and terrestrial plant debris incorporated within a matrix of amorphous organic matter and clumped aggregates of endogenic calcite (Fig. 4.4a+d).

4.4 Detrital layer geochemistry

Detrital layer geochemistry differs within the lake basin (Fig. 4.5). In the northern part of the lake basin (Fig. 4.5a) detrital layers exhibit high values in Ti count rates (proxy for siliciclastic matter) and low values of Mg (proxy for dolomitic components). The predominantly siliciclastic composition corroborates the Flysch zone (Fig. 4.1) as main source of detrital material. In contrast, the element composition of detrital layers in the southern part of the basin (Fig. 4.5b) is more complex. Four layers exhibit clear peaks in Ti, thus pointing to the Flysch zone as main source region (DL 4, 12, 18, 19), whereas two layers show increased Mg counts indicating the Northern Calcareous Alps as sediment source (DL 10, 16). One layer shows both higher Ti and Mg values indicating a mixture of material from both sources (DL 9).

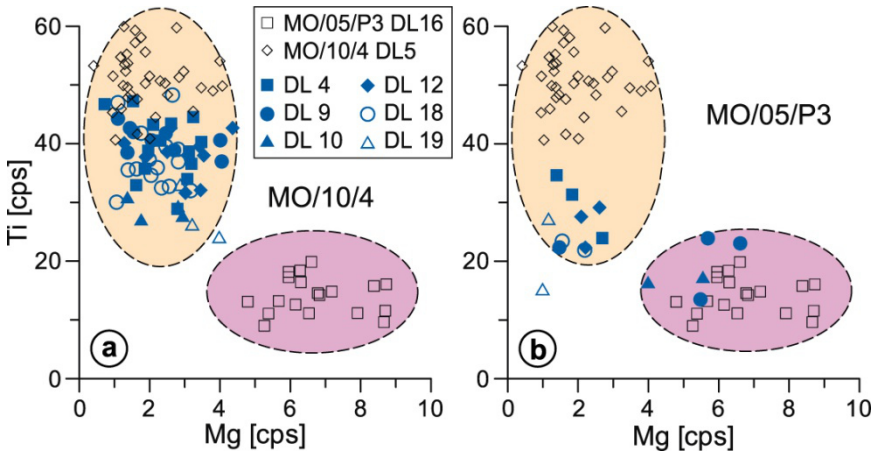

Figure 5. Micro-XRF counts of Ti and Mg within flood layers (blue symbols): (a) in the proximal sediment core MO/10/4 and (b) in the distal master core MO/05/P4. Reference layers for source identification (black symbols) are DL 5 triggered by a local flood in the northern Flysch sub-catchment and DL 16 triggered by a debris flow event in the southern sub-catchment in the Northern Calcareous Alps. Circles indicate areas representative for the two sub-catchments; yellow: Flysch Zone, pink: Northern Calcareous Alps.

4.5 Intra-basin distribution of detrital layers

Based on independent varve counting in all 12 investigated sediment cores, intra-basin correlation of detrital layers has been performed (Fig. 4.3) to identify the spatial distribution of each individual detrital layer within the lake basin and disentangle between the three potential point sources for suspended sediment supply, the Griesler and Wangauer Ache discharging from the West and from the East into the northern part of the basin where the shape of the lake makes a kink and the Kienbach creek discharging from the South into the southern part of the basin.

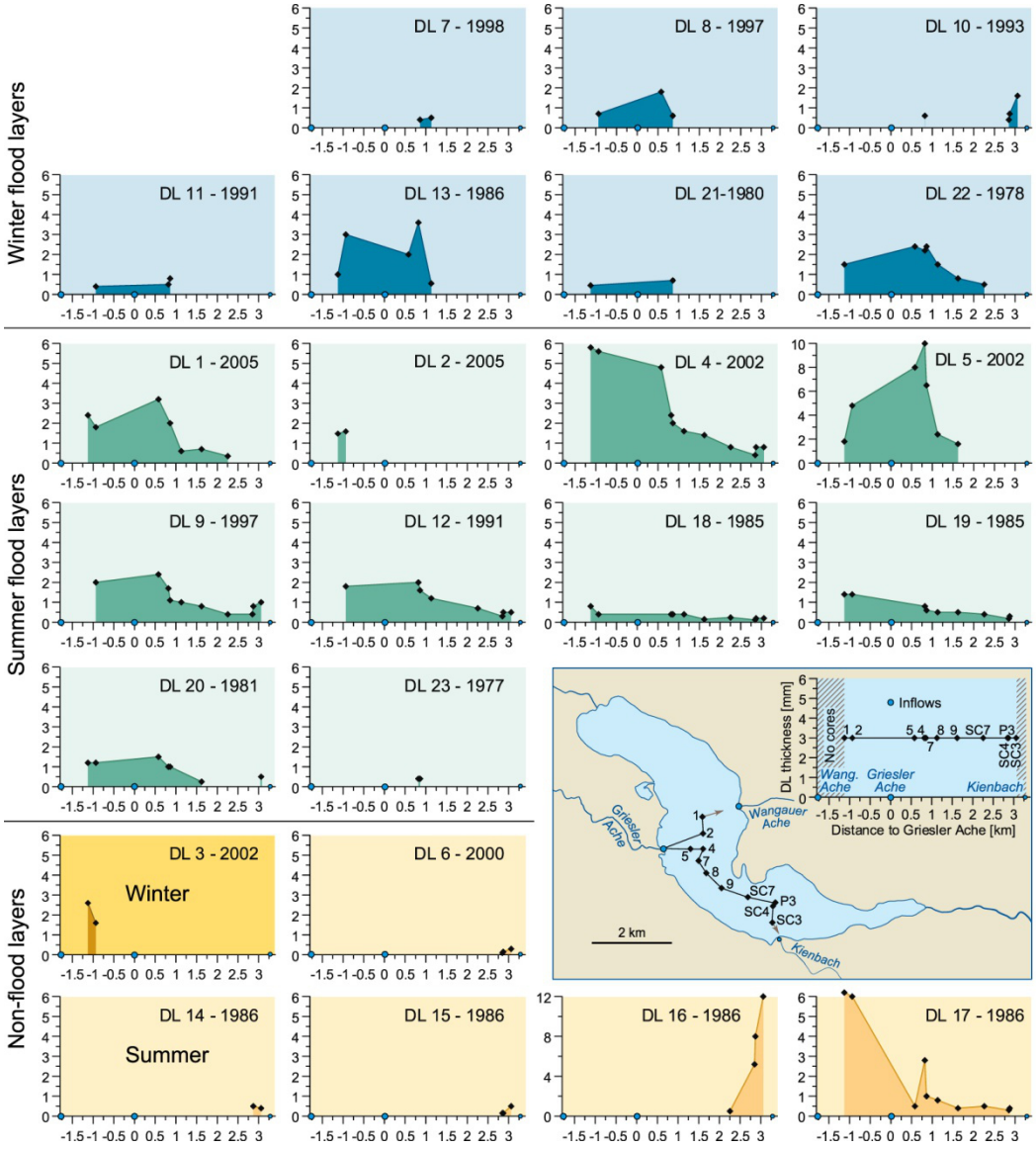

Figure 6. Spatial distribution of detrital layers within Lake Mondsee: layers triggered by floods in winter and summer and layers not related to floods. Sampling points are arranged along transects as shown in the map.

The investigated sediment interval from 1976 to 2005 includes 27 detrital layers (Tab. 4.1). Four layers with a thickness from 0.2 to 4.5 mm were only found each in one sediment core at the most proximal locations close to the river inflows (MO/10/2: 2 layers, MO/10/7 and MO/07/SC3: 1 layer each) and likely reflect local reworking of unconsolidated delta material. The remaining 23 detrital layers have been correlated within the investigated part of the basin (Fig. 4.3).

Sediment cores located near the inflow of the main tributary Griesler Ache (ca. 0.8 km) contain the highest number and thickest detrital layers (MO/10/4: 13 layers, max. 10 mm, MO/10/7: 15 layers, max. 6.5 mm) indicating the Griesler Ache as the main source of detrital material. Towards the depocentre of the lake the number of detrital layers decreases and these layers commonly are thinner (MO/07/SC7 (2.3 km): 8 layers, max. 0.8 mm). Besides this common proximal-distal pattern of sediment flux, four detrital layers (DL 4, 9, 10, 12) show a slightly increasing thickness towards the Kienbach inflow suggesting an additional sediment flux occurring from the Kienbach creek in the South contemporaneously to the sediment flux from the main tributary (Fig. 4.6). Further four detrital layers (DL 6, 14-16), which are all matrix-supported, have been only deposited in the southern part of the basin indicating the Kienbach creek as the exclusive sediment source (Fig. 4.6).

The distribution of suspended detrital matter within the lake basin after a flood apparently is dependent from the season in which the flood occurred. Whereas six of the seven winter floods are only recorded in cores within 1.5 km distance from the Griesler Ache and Wangauer Ache river mouths mainly as matrix-supported layers (90%), summer flood layers are much wider distributed within the lake basin (Fig. 4.6). From the 11 summer layers found in proximal cores near the Griesler Ache inflow (MO/10/4+7), eight layers are distributed over a distance of 1.6 km (MO/10/9) and six layers even further South to the location of the long master core in 2.9 km distance. The microfacies of these layers changes from graded layers at proximal sites (82% in MO/10/4+7) to silt/clay layers at distal sites (50% in MO/10/8, 63% in MO/10/9, 91% in MO/07/SC7). Three of the very fine-grained silt/clay layers in the distal master core (DL 12, 18, 19) could only be identified as detrital layers by correlation with the proximal core sequences. These layers have been added to the previously published long flood layer chronology (Swierczynski *et al.*, 2012 and 2013).

4.6 Detrital layers vs. instrumental data

To investigate the effects of river discharge on detrital layer formation, all 23 detrital layers occurring between 1976 and 2005 in at least two of the sediment cores have been compared to discharge data of the gauged main tributary river, Griesler Ache, and precipitation data of the three sub-catchments of Lake Mondsee (Fig. 4.7). This event-based comparison with instrumental data is

possible due to the determination of the flood seasons in the sediment record by micro-stratigraphical methods. 17 detrital layers (74%) correspond to events of elevated runoff in the Griesler Ache ranging in maximum daily discharge (Q_d) from 24 to 83 m^3s^{-1}. 12 of these layers (70%) correlate to strong floods exceeding 40 m^3s^{-1}. This runoff value was exceeded 13 times in the studied time interval and in all except one case this discharge resulted in the deposition of a detrital layer (92%). The likelihood for detrital layer deposition sharply decreases for lower flood amplitudes and is only 12% for floods with a daily discharge of 30-40 m^3s^{-1}.

Ten of the 17 floods, led to detrital layer deposition, occurred in summer of which 90% relate to intense precipitation (P) > 80 mm d^{-1} and associated hourly peak discharges (Q_h) > 60 m^3s^{-1} (Tab. 4.2). Detrital layers which formed after summer floods commonly are widely distributed in six to 12 sediment cores, except for one flood in July 1977 of which corresponding detrital layers have been found only in two proximal cores (Fig. 4.6). Five of the remaining seven floods occurred in spring (March-April) and two in winter (Tab. 4.2) all related to rain events exceeding 50 mm d^{-1} and commonly less extreme peak discharges (57% < 60 m^3s^{-1}) leading to detrital layer deposition in two to six cores.

For six detrital layers which occur in few cores either close to the Kienbach creek in the South (DL 6, 14-16) or close to the Wangauer Ache in the North (DL 3), neither coinciding discharge events in the Griesler Ache nor precipitation events in any sub-catchment have been measured. Therefore, local erosion or reworking processes rather than regional-scale flood events are assumed to have caused the formation of these layers. This has been proven for layer DL 16, which was triggered by a documented debris flow in the Kienbach valley (Swierczynski *et al.*, 2009). Among these detrital layers, which are not related to floods, only DL 17 exhibits a wider distribution in the lake basin and has been found in 11 cores. The thickness distribution of this layer within the basin points to the Wangauer Ache as source (Fig. 4.6). In summary, 17 of 23 detrital layers correspond to floods of the Griesler Ache (Fig. 4.7), and six layers are related to local events.

Besides detrital layers triggered by other processes than regional floods, flood layer records might be biased by missing flood layers, i.e. floods that did not result in deposition of a detrital layer. For the studied interval, only one major Griesler Ache flood in November 1979 (Q_d = 41.9 m^3s^{-1}) did not result in detrital layer deposition in any of the sediment cores (Tab. 4.2). However, the completeness of individual sediment cores with respect to flood layer deposition distinctly varies within the lake basin. Some layers are not perceptible in individual sediment cores, either due to predominantly clastic background sedimentation at the most proximal sites (e.g. MO/10/5) or sediment intervals with a less well preserved varve structure (Tab. 4.1). Such individual gaps were bridged by integrating neighbouring sediment cores to form composite profiles providing a more representative flood layer record (Fig. 4.7).

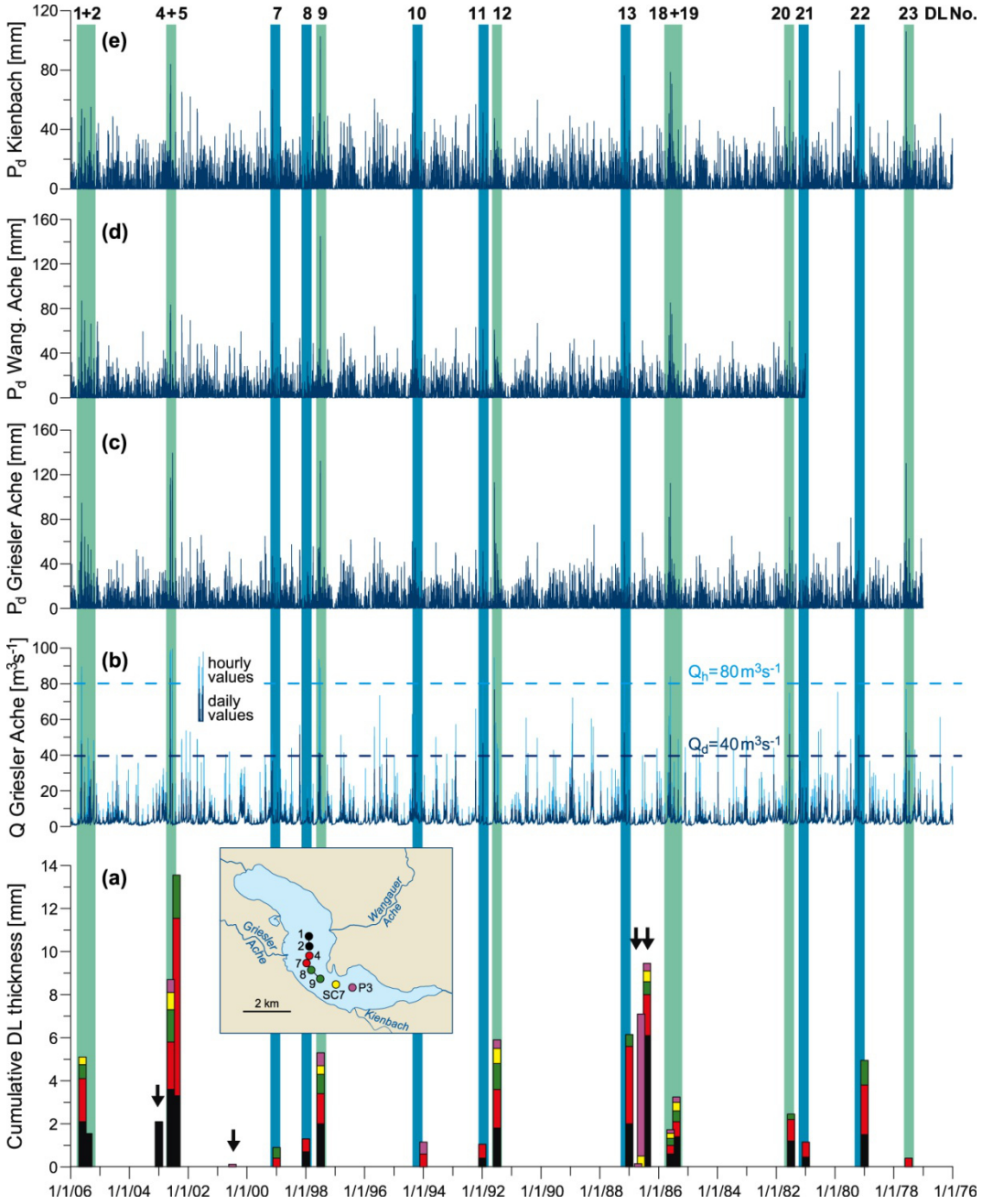

Figure 7. Mondsee detrital layer record compared to instrumental time series 1976-2005: (a) Layer thickness in five composite profiles (see map), (b) Griesler Ache daily and hourly discharge, (c-e) precipitation in the three main sub-catchments (Griesler Ache: Thalgauberg rain gauge, Wangauer Ache: Oberwang, Kienbach: Scharfling. Vertical bars: coincidence of detrital layer deposition and floods in winter (blue) and summer (green); black arrows: detrital layers not related to floods; horizontal dashed lines: empirical runoff thresholds for triggering detrital layers in Lake Mondsee.

Sediment cores in the proximal part of the basin, 0.9 km apart from the Griesler Ache inflow (MO/10/4+7), contain 16 of the total 17 flood layers, whereas towards distal direction the number of identified floods decreases: 11 layers (65%) are transported over a distance of 1.5 km (MO/10/8+9) and six layers (35%) to the master core in the distal southern part of the basin in a distance of 2.9 km to the Griesler Ache inflow. Four of the six floods, recorded in the master core, are the

strongest summer floods in the investigation period in terms of intensity (Q_h > 80 m^3s^{-1}) and duration (Q_d > 40 m^3s^{-1} for at least 2 days). The other two flood layers in the master record were triggered by a summer flood below the threshold (DL 18; Q_d = 30.3 m^3s^{-1}) and a local spring precipitation event in the Kienbach catchment (DL 10; P = 86.2 mm d^{-1}).

5 Discussion

Detrital layers in lake sediments commonly are considered as flood indicators (Siegenthaler and Sturm, 1991; Gilli *et al.*, 2013). However, there is still a lack of knowledge about the completeness of palaeoflood records and how discharge and precipitation control the formation and thickness of flood layers (Gilli *et al.*, 2013). An important aspect for interpreting the number and thickness of detrital layers deposited after flood events certainly is the coring location with respect to the inflowing suspended matter (Czymzik *et al.*, 2013). Here, we address these issues in a detailed case study for the Lake Mondsee sediment record by a comprehensive methodological approach combining multiple-core analyses with a calibration of detrital layers based on instrumental flood data. The precise chronology of varved sediment records gives the unique opportunity of such an individual event-based comparison of sedimentological and instrumental flood records (Schiefer *et al.*, 2006; Chutko and Lamoureux, 2008; Czymzik *et al.*, 2010). Reconstruction of flood layer distribution within the lake basin through multiple core analyses provides complementary information about depositional processes (Sturm and Matter, 1978; Gilbert *et al.*, 2006; Schiefer, 2006; Schiefer *et al.*, 2011; Kämpf *et al.*, 2012a) and, in combination with sediment geochemistry, about sediment source areas (Swierczynski *et al.*, 2009; Simonneau *et al.*, 2013).

An important factor for interpreting detrital layers as flood deposits is the process of suspended sediment distribution within the basin either though underflows (hyperpycnal flows) or interflows (mesopycnal flows). Based on our detailed intra-basin correlation we assume that graded and matrix supported layers represent hyperpycnal flow deposits whereas silt/clay layers which are mostly very thin and almost evenly distributed over the lake basin represent mesopycnal flow deposits. Hyperpycnal flow deposits are rarely found in the depocentre of Lake Mondsee (MO/07/SC7 in Tab. 4.1); only one graded layer occurs during the studied time interval, whereas all other detrital layers appear as silt/clay layers. However, since all silt/clay layers in the depocentre can be unambiguously correlated to graded layers in proximal cores by their micro-stratigraphic position within the varved sediment sequence, we infer a separation of the suspended sediment plumes triggered by regional flooding into hyperpycnal flows confined to the near delta area (c. 1.5 km) and mesopycnal flows which are distributed to more distal parts of the lake basin. In this respect Lake Mondsee is different from

larger peri-alpine lakes like, for example, lakes Bourget and Brienz, where thick turbidites resulting from underflows have been found in the entire depocentre (Sturm and Matter, 1978; Arnaud *et al.*, 2005; Chapron *et al.*, 2005). Besides the smaller size of Lake Mondsee and its main tributary, the specific shape of the lake basin and the location of the main inflow with respect to the main water flow direction, as above described in the section study site, likely influences the amount of suspended matter influx and its distribution within the lake basin.

Table 2. Comparison of the detrital layer record and instrumental time series for the investigation period 1976-2005. Instrumental data include maximum daily and hourly runoff in the main tributary, Griesler Ache, daily precipitation sums in the catchments of the main and secondary tributaries and weather regime data from Gerstengarbe and Werner (2005).

Sediment data					Hydrological data					Max. daily precipitation			
Varve year	Varve season	DL No.	N Cores	Cum. Thickness [mm]	Date of max. runoff	Daily runoff [m^3s^{-1}]	Hourly runoff [m^3s^{-1}]	Flood duration [d] [> 40 m^3s^{-1}]	[> 20 m^3s^{-1}]	Thalgauberg [mm]	Oberwang [mm]	Scharfling [mm]	Weather type
2005	su	1	7	11.1	8/16/2005	**46.3**	**89.6**	1	1	**94.7**	**87.0**	54.0	WZ
2005	su	2	2	3.1	7/11/2005	24.8	33.6	0	1	64.4	69.5	48.0	TRM
2002	*wi*	*3*	*2*	4.2	*11/4/2002*	*20.5*	*32.6*	*0*	*1*	*32.7*	*42.5*	*32.8*	
2002	su	4	12	25.0	8/12/2002	**83.2**	**112.8**	2	3	**117.2**	**83.5**	**84.0**	TM
2002	su	5	8	39.5	7/16/2002	24.2	**99.6**	0	1	**139.5**	30.0	19.5	TRM
2000	*su*	*6*	*3*	0.6	*8/7/2000*	*17.8*	*45.2*	*0*	*0*	*50.8*	*46.6*	*44.3*	
1998	wi	7	2	0.9	2/21/1999	36.8	52.0	0	3	46.9	67.5	67.0	NWZ
1997	wi	8	3	3.1	3/17/1998	**51.7**	56.9	1	3	52.8	53.5	35.2	NWZ
1997	su	9	11	13.4	7/6/1997	**41.0**	**89.0**	2	3	**132.4**	**145.0**	**102.7**	TRW
1993	wi	10	4	3.3	4/18/1994	**40.4**	**62.5**	1	1	54.5	**92.8**	**86.2**	TM
1991	wi	11	3	1.7	12/23/1991	**46.8**	**82.6**	1	2	51.2	61.5	51.6	WZ
1991	su	12	9	10.2	8/2/1991	**76.8**	**94.8**	3	4	**113.0**	61.0	47.7	HFA
1986	wi	13	6	11.8	3/1/1987	**52.7**	**81.4**	3	4	60.0	68.0	76.4	WW
1986	*su*	*14*	*2*	0.9	-								
1986	*su*	*15*	*3*	0.8	-								
1986	*su*	*16*	*4*	25.7	*7/18/1986*	*11.0*	*43.8*	*0*	*0*	*68.0*	*51.3*	*42.0*	
1986	*su*	*17*	*11*	19.4	*6/18/1986*	*4.3*	*39.1*	*0*	*0*	*45.2*	*31.5*	*19.8*	
1985	su	18	10	3.4	8/26/1985	30.3	**62.0**	0	2	**82.2**	56.2	50.8	TRM
1985	su	19	10	6.9	8/6/1985	**51.5**	**84.1**	2	2	**112.4**	**85.5**	78.7	TRM
1981	su	20	8	7.4	7/19/1981	**51.8**	**74.8**	2	3	**82.2**	69.0	73.0	TRM
1980	wi	21	3	1.5	3/12/1981	36.7	53.1	0	4	25.2	25.3	30.0	SWZ
				-	11/27/1979	**41.9**	**75.5**	1	2	59.1	no data	54.2	BM
1978	wi	22	7	12.2	3/12/1979	**51.3**	**69.4**	2	2	52.1	no data	57.5	WZ
1977	su	23	2	0.8	7/31/1977	**52.7**	**77.0**	1	2	**130.2**	no data	**106.0**	NEZ

Extreme values of hydrological parameters are written in bold (daily runoff > 40 m3s-1, hourly runoff > 60 m3s-1, daily precipitation > 80 mm), detrital layers not related to floods are written in italic. Abbreviations for sediment data: DL No.: detrital layer number, N cores: amount of cores containing the layer, Cum. Thickness: cumulative detrital layer thickness added up over all cores, acronyms for weather types (Gerstengarbe and Werner, 2005): WZ: westerly cyclonic, TRM: low pressure trough over Central Europe, TM: low pressure cell over Central Europe, NWZ: north-westerly cyclonic, HFA: high pressure cell over Fennoscandia anticyclonic, WW: angular westerly, SWZ: south-westerly cyclonic, BM: high pressure ridge over Central Europe, NEZ: north-easterly cyclonic.

5.1 Reconstructing flood frequencies

The comparison with instrumental flood data revealed an empirical discharge threshold for detrital layer deposition in Lake Mondsee sediments of about 40 m^3s^{-1} mean daily discharge (Fig. 4.7). Above this threshold detrital layers are formed in at least two sediment cores in the lake basin. However, we observe clear variations of this threshold for different locations within the lake due to the

different distance from the inflow of suspended matter. In the distal lake basin the threshold is even better defined by maximum peak discharge and flood duration rather than by mean daily discharge. The long master core predominately records floods exceeding 80 m^3s^{-1} peak discharge and a daily mean of 40 m^3s^{-1} lasting for at least two days. In addition, we found that not all detrital flood layers have been formed at all core locations, not only because of different distances from the inflow source, but also due to variable distribution of suspended sediment loads within the lake. In summary, flood layer time series obtained from single cores indeed might be biased by so-called 'missing' flood layers so that such flood reconstructions must be considered as minimum flood estimates.

Possible explanations for missing layers include erosion by hyperpycnal flows (Mangili *et al.*, 2005; Schiefer, 2006) and sediment focusing by meandering (Gilbert *et al.*, 2006) or spatially limited hyperpycnal flows (Lamoureux, 1999). Alternative explanations are related to an uneven distribution of suspended matter within the basin especially during mesopycnal flow transport. A previously underestimated factor in this respect is the season of flooding. For Lake Mondsee we demonstrate that summer detrital layers are much wider distributed within the basin compared to winter flood layers which are spatially confined to sites proximal to the inflow even during strong winter floods (Fig. 4.6). This might be explained by summer stratification favouring long-distance transport of fine-grained suspended matter in the upper water column to the depocentre by mesopycnal flows (Sturm and Matter, 1978; Desloges and Gilbert, 1994; Schiefer, 2006; Hodder *et al.*, 2007). Moreover, lake internal currents, recorded during an ongoing monitoring study in Lake Mondsee (Mueller *et al.*, 2013), could have a potential effect on mesopycnal flows (Sturm and Matter, 1978; Giovanoli and Lambert, 1985; Schiefer, 2006). Although the generation of lake internal currents might be specific in Lake Mondsee (Mueller *et al.*, 2013) because of the characteristic basin morphology and the position of the discharging river inflows, an influence of internal currents for sediment distribution must be considered for all larger lake systems.

In addition to missing layers as a bias for interpreting long palaeoflood time series, there is also the possibility of additional detrital layers, which are not related to regional floods and thus may lead to an overestimation of flood numbers. In Lake Mondsee, such non flood-triggered layers are formed by two different mechanisms: (i) debris flows deriving from the steep-sided Kienbach valley in the southern sub-catchment (Swierczynski *et al.*, 2009) and (ii) reworking of unconsolidated sediment from the deltas and slopes through wave action and sediment instabilities. Debris flow deposits can be clearly distinguished from flood layers based on the exclusively dolomitic sediment composition (Fig. 4.5) and coarser detrital grain sizes. Reworked detrital material deposited around the river deltas commonly did not form distinct layers and, therefore, can be also distinguished from flood deposits. Only in one case, a distinct and widespread detrital layer with a similar appearance like other flood layers (DL 17, Fig. 4.6)

has formed without a corresponding discharge peak in the Griesler Ache. This layer is not distinguishable from common flood layers. Intra-basin correlation enabled to trace this layer to the Wangauer Ache stream. Since no enhanced precipitation is recorded in the Wangauer Ache catchment during that time (Fig. 4.7), we assume a local erosion event either in the stream bed or from the subaquatic slopes.

Based on the abovementioned evidences, we can state that the long master core located in the distal southern basin completely records the strongest summer floods defined as peak discharge (80 m^3s^{-1}) and flood duration (2 days > 40 m^3s^{-1}). In addition to the earlier published flood layer record based on only the master core (Swierczynski *et al.*, 2012 and 2013), we were able to identify three extremely thin flood layers (DL 12, 18, 19) through the multi-core approach. The amounts of detrital material transported to this distal site were so low, that we could identify them only through tracing flood material from the proximal site. The preferential deposition of summer flood layers can be explained by the effect of lake stratification favouring wide distribution of suspended matter through mesopycnal flows. Local erosion events can be, in most cases, clearly distinguished from flood deposits by multiple core micro-facies and micro-XRF analyses. Obviously, the empirical threshold must be considered as an approximation since also two low amplitude floods triggered the formation of detrital layers.

5.2 Reconstructing flood amplitudes

Besides establishing long time series of flood frequencies, it is challenging to reconstruct also amplitudes of palaeofloods. First attempts applied flood layer thickness as proxy for flood amplitudes (Brown *et al.*, 2000; Wilhelm *et al.*, 2013; Wirth *et al.*, 2013) based on the concept that sediment flux in the lake is directly related to river discharge as has been demonstrated in several pro-glacial lakes (Desloges and Gilbert, 1994; Schiefer *et al.*, 2006; Hodder *et al.*, 2007; Chutko and Lamoureux, 2008; Schiefer *et al.*, 2011). Although in agreement with this concept, most of the thickest flood layers in the Mondsee sediment record (1 to 5 mm; Fig. 4.7) indeed were triggered by the strongest flood events (1991, 1997, 2002), our calibration demonstrates that the assumed relation between flood amplitude and layer thickness is not generally valid but shows clear differences depending from the particular core position within the lake basin. This is obvious from highly variable linear correlation coefficients (Tab. 4.3). Reasons for these variations are non-linear components influencing layer thickness in different ways. For example, layer thickness in the distal southern part of the lake does not correlate to flood amplitudes ($r^2(Q_h) = 0.22$), because of additional sediment supply from the local Kienbach creek (Figs. 5 and 6) into this part of the basin. The proximal zone is generally more susceptible for local sediment mobilization

events in the catchment or from the slopes which can cause thick detrital layers (DL 5, 16, 17) as has been also shown for other lake sediment records (Czymzik *et al.*, 2010; Kämpf *et al.*, 2012b). For the Lake Mondsee record, a significant linear correlation of layer thickness and flood amplitude is only revealed for the depocentre ($r^2(Q_h) = 0.77$), which is far enough from additional local sediment sources and receives sediment supply only after the strongest floods crossing a certain threshold.

Table 3. Linear correlation of detrital layer thickness from composite sediment profiles with daily (Q_d) and hourly runoff maxima (Q_h) in the main tributary Griesler Ache.

	MO/10/1+2	MO/10/4+7	MO/10/8+9	MO/07/SC7	MO/ P3+SC4
n flood layers	14	16	11	6	6
r^2 (Q_d)	0.08	0.03	0.02	0.96	0.13
p (Q_d)	>0.1	>0.1	>0.1	0.001	>0.1
r^2 (Q_h)	0.48	0.28	0.46	0.76	0.22
p (Q_h)	0.04	>0.1	0.08	0.04	>0.1

In addition to processes observed at Lake Mondsee, other processes are assumed to influence flood layer thickness including soil moisture and vegetation cover which affect runoff generation (Merz and Blöschl, 2009) and erosivity of soil and surface sediments and thereby, the amount of suspended material transported in the streams (Dugan *et al.*, 2009; López-Tarazón *et al.*, 2010). Although these factors can also vary on short time scales, they commonly work on longer time scales through soil evolution, climatic controlled land-cover changes and human impact (Giguet-Covex *et al.*, 2011; Arnaud *et al.*, 2012), and thus result in a complex non-linear relation of flood amplitude and layer thickness in centennial to millennial scale lake sediment records. Due to the limited calibration period of the present study, these long-term processes are out of the observational range and cannot be addressed here.

In summary, the relation between detrital layer thickness and flood amplitude depends on a complex interaction of linear and non-linear factors controlling discharge and suspended sediment transport in tributary streams and sediment distribution within the lake and shows a distinct spatial heterogeneity within the lake basin. Deciphering these processes can be at least partly achieved by multiple sediment core analyses and calibration of sediment with meteorological and hydrological data.

6 Conclusions

The applied dual calibration approach for flood layer deposition in a lake sediments combining multi-core micro-facies analyses and calibration with

instrumental data turned out suitable to decipher processes controlling flood layer formation, thereby, fostering an improved interpretation of long flood layer time series derived from lake sediments. This approach allowed identifying missing layers or additional, non-flood triggered detrital layers at individual core locations. In addition, empirical flood amplitude thresholds for the formation of flood layers have been assessed and proven to be specific for different coring locations. This, in turn, is important information for defining the most suitable coring locations for future lake sediment investigations aiming at flood reconstructions. Our study further demonstrates that the season in which a flood occurs influences the distribution of detrital material within the lake basin, possibly because of the state of lake water stratification and/or internal water currents. However, these assumptions remain speculative and need to be tested by extending the observation through in-lake monitoring of suspended matter distribution and deposition.

The results of this study provide a more robust interpretation of the long flood time series from Lake Mondsee and allow to better estimate uncertainties. In more general, we contribute to the discussion if and how flood layer thickness can be applied as proxy for flood amplitude by demonstrating that in certain circumstances a relationship between layer thickness and flood amplitude exists. However, this relationship can be strongly overprinted by non-linear components and is spatially different even within one lake basin. Therefore, reconstructing flood amplitudes still remains a major challenge for palaeoflood research in lake sediments. Even if our results obviously are in parts site-specific, we consider the dual calibration approach for flood layers as a suitable tool also for other lake records. Ideally, it should be complemented by observation of in-situ sedimentation through in-lake monitoring.

Acknowledgements. This study contributes to the Potsdam Research Cluster for Georisk Analysis, Environmental Change and Sustainability (PROGRESS) part A.3 ‘Extreme events in geoarchives’ funded by the German Federal Ministry for Education and Research (BMBF). We especially thank Richard Niederreiter (UWITEC) and Hannes Höllerer (University of Innsbruck) for their help during sediment sampling, Michael Köhler (MK Factory), Dieter Berger and Gabriele Arnold (both Helmholtz Centre Potsdam GFZ) for the preparation of thin sections and Brigitte Richert (Helmholtz Centre Potsdam GFZ) for performing µ-XRF measurements. Andreas Hendrich and Manuela Dziggel helped with the figures. Precipitation and discharge data sets were supplied by the hydrographic services of Upper Austria and Land Salzburg. Temperature data for the climate station of Mondsee were provided by the Central Institute for Meteorology and Geodynamics Austria (ZAMG). We thank Dr. Kyle Hodder and an anonymous reviewer for constructive comments which helped to improve the manuscript.

References

Arnaud F, Revel M, Chapron E, Desmet M, Tribovillard N. 2005. 7200 years of Rhone river flooding activity in Lake Le Bourget, France: a high-resolution sediment record of NW Alps hydrology. *Holocene* **15**: 420-428.

Arnaud F, Révillon S, Debret M, Revel M, Chapron E, Jacob J, Giguet-Covex C, Poulenard J, Magny M. 2012. Lake Bourget regional erosion patterns reconstruction reveals Holocene NW European Alps soil evolution and paleohydrology. *Quaternary Science Reviews* **51**: 81-92.

Brauer A, Casanova J. 2001. Chronology and depositional processes of the laminated sediment record from Lac d'Annecy, French Alps. *Journal of Paleolimnology* **25**: 163-177.

Brauer A, Dulski P, Mangili C, Mingram J, Liu J. 2009. The potential of varves in high-resolution paleolimnological studies. *PAGES news* **17**: 96-98.

Brown SL, Bierman PR, Lini A, Southon J. 2000. 10 000 yr record of extreme hydrologic events. *Geology* **28**: 335-338.

Chapron E, Arnaud F, Noël H, Revel M, Desmet M, Perdereau L. 2005. Rhone River flood deposits in Lake Le Bourget: a proxy for Holocene environmental changes in the NW Alps, France. *Boreas* **34**: 404-416.

Chutko KJ, Lamoureux SF. 2008. Identification of coherent links between interannual sedimentary structures and daily meteorological observations in Arctic proglacial lacustrine varves: potentials and limitations. *Canadian Journal of Earth Sciences* **45**: 1-13.

Cockburn J, Lamoureux S. 2008. Inflow and lake controls on short-term mass accumulation and sedimentary particle size in a High Arctic lake: implications for interpreting varved lacustrine sedimentary records. *Journal of Paleolimnology* **40**: 923-942.

Crookshanks S, Gilbert R. 2008. Continuous, diurnally fluctuating turbidity currents in Kluane Lake, Yukon Territory. *Canadian Journal of Earth Sciences* **45**: 1123-1138.

Czymzik M, Brauer A, Dulski P, Plessen B, Naumann R, von Grafenstein U, Scheffler R. 2013. Orbital and solar forcing of shifts in Mid- to Late Holocene flood intensity from varved sediments of pre-alpine Lake Ammersee (southern Germany). *Quaternary Science Reviews* **61**: 96-110.

Czymzik M, Dulski P, Plessen B, Grafenstein v, Naumann R, Brauer A. 2010. A 450-year record of spring/summer flood layers in annually laminated sediments from Lake Ammersee (Southern Germany). *Water Resour. Res.*

Desloges JR, Gilbert R. 1994. Sediment source and hydroclimatic inferences from glacial lake sediments: the postglacial sedimentary record of Lillooet Lake, British Columbia. *J. Hydrol.* **159**: 375-393.

Dokulil M, Skolaut C. 1986. Succession of phytoplankton in a deep stratifying lake: Mondsee, Austria. *Hydrobiologica* **138**: 9-24.

Dugan HA, Lamoureux SF, Lafreniere MJ, Lewis T. 2009. Hydrological and sediment yield response to summer rainfall in a small high Arctic watershed. *Hydrological Processes* **23**: 1514-1526.

Gerstengarbe F, Werner P, 2005. Katalog der Großwetterlagen Europas (1881–2004) nach Paul Hess und Helmut Brezowsky. Potsdam Institute For Climate Impact Research, Potsdam: 153.

Giguet-Covex C, Arnaud F, Poulenard J, Disnar JR, Delhon C, Francus P, David F, Enters D, Rey PJ, Delannoy JJ. 2011. Changes in erosion patterns during the

Holocene in a currently treeless subalpine catchment inferred from lake sediment geochemistry (Lake Anterne, 2063 m a.s.l., NW French Alps): The role of climate and human activities. *Holocene* **21**: 651-665.
Gilbert R, Crookshanks S, Hodder KR, Spagnol J, Stull RB. 2006. The record of an extreme flood in the sediments of montane Lillooet Lake, British Columbia: Implications for paleoenvironmental assessment. *Journal of Paleolimnology* **35**: 737-745.
Gilli A, Anselmetti F, Glur L, Wirth S. 2013. Lake Sediments as Archives of Recurrence Rates and Intensities of Past Flood Events, In: *Dating Torrential Processes on Fans and Cones*, Schneuwly-Bollschweiler M, Stoffel M, Rudolf-Miklau F (eds.). Springer Netherlands; 225-242.
Gilli A, Anselmetti FS, Ariztegui D, McKenzie JA. 2003. A 600-year sedimentary record of flood events from two sub-alpine lakes (Schwendiseen, Northeastern Switzerland). *Eclogae geol. Helv.* **96**: 49-58.
Giovanoli F, Lambert A. 1985. Die Einschichtung der Rhone im Genfersee: Ergebnisse von Strömungsmessungen im August 1983. *Aquatic Sciences - Research Across Boundaries* **47**: 159-178.
Glur L, Wirth SB, Büntgen U, Gilli A, Haug GH, Schär C, Beer J, Anselmetti FS. 2013. Frequent floods in the European Alps coincide with cooler periods of the past 2500 years. *Sci. Rep.* **3**.
Hodder K, Gilbert R, Desloges J. 2007. Glaciolacustrine varved sediment as an alpine hydroclimatic proxy. *Journal of Paleolimnology* **38**: 365-394.
Kämpf L, Brauer A, Dulski P, Feger K-H, Jacob F, Klemt E. 2012a. Sediment imprint of the severe 2002 summer flood in the Lehnmühle reservoir, eastern Erzgebirge (Germany). *E&G - Quaternary Science Journal* **61**: 3-15.
Kämpf L, Brauer A, Dulski P, Lami A, Marchetto A, Gerli S, Ambrosetti W, Guilizzoni P. 2012b. Detrital layers marking flood events in recent sediments of Lago Maggiore (N. Italy) and their comparison with instrumental data. *Freshwater Biology* no-no.
Klee R, Schmidt R. 1987. Eutrophication of Mondsee (Upper Austria) as indicated by the diatom stratigraphy of a sediment core. *Diatom Research* **2**: 55-76.
Lamoureux S. 1999. Spatial and interannual variations in sedimentation patterns recorded in nonglacial varved sediments from the Canadian High Arctic. *Journal of Paleolimnology* **21**: 73-84.
Lamoureux S. 2000. Five centuries of interannual sediment yield and rainfall-induced erosion in the Canadian High Arctic recorded in lacustrine varves. *Water Resour. Res.* **36**: 309-318.
Lauterbach S, Brauer A, Andersen N, Danielopol DL, Dulski P, Huls M, Milecka K, Namiotko T, Obremska M, Von Grafenstein U, Declakes P. 2011. Environmental responses to Lateglacial climatic fluctuations recorded in the sediments of pre-Alpine Lake Mondsee (northeastern Alps). *Journal of Quaternary Science* **26**: 253-267.
Lauterbach S, Chapron E, Brauer A, Hüls M, Gilli A, Arnaud F, Piccin A, Nomade J, Desmet M, von Grafenstein U, Participants D. 2012. A sedimentary record of Holocene surface runoff events and earthquake activity from Lake Iseo (Southern Alps, Italy). *The Holocene*.
López-Tarazón JA, Batalla RJ, Vericat D, Balasch JC. 2010. Rainfall, runoff and sediment transport relations in a mesoscale mountainous catchment: The River Isábena (Ebro basin). *Catena* **82**: 23-34.

Mangili C, Brauer A, Moscariello A, Naumann R. 2005. Microfacies of detrital event layers deposited in quaternary varved lake sediments of the Pianico-Sellere Basin (northern Italy). *Sedimentology* **52**: 927-943.

Merz R, Blöschl G. 2009. A regional analysis of event runoff coefficients with respect to climate and catchment characteristics in Austria. *Water Resour. Res.* **45**: W01405.

Mudelsee M, Borngen M, Tetzlaff G, Grunewald U. 2004. Extreme floods in central Europe over the past 500 years: Role of cyclone pathway "Zugstrasse Vb". *J. Geophys. Res.-Atmos.* **109**.

Mueller P, Thoss H, Kaempf L, Güntner A. 2013. A Buoy for Continuous Monitoring of Suspended Sediment Dynamics. *Sensors* **13**: 13779-13801.

Parajka J, Kohnová S, Bálint G, Barbuc M, Borga M, Claps P, Cheval S, Dumitrescu A, Gaume E, Hlavčová K, Merz R, Pfaundler M, Stancalie G, Szolgay J, Blöschl G. 2010. Seasonal characteristics of flood regimes across the Alpine–Carpathian range. *J. Hydrol.* **394**: 78-89.

Petrow T, Zimmer J, Merz B. 2009. Changes in the flood hazard in Germany through changing frequency and persistence of circulation patterns. *Nat. Hazards Earth Syst. Sci.* **9**: 1409-1423.

Schiefer E. 2006. Depositional Regimes and Areal Continuity of Sedimentation in a Montane Lake Basin, British Columbia, Canada. *Journal of Paleolimnology* **35**: 617-628.

Schiefer E, Gilbert R, Hassan MA. 2011. A lake sediment-based proxy of floods in the Rocky Mountain Front Ranges, Canada. *Journal of Paleolimnology* **45**: 137-149.

Schiefer E, Menounos B, Slaymaker O. 2006. Extreme sediment delivery events recorded in the contemporary sediment record of a montane lake, southern Coast Mountains, British Columbia. *Canadian Journal of Earth Sciences* **43**: 1777-1790.

Schmidt R. 1991. Recent re-oligotrophictaion in Mondsee (Austria) as indicated by sediment diatom and chemical stratigraphy. *Verh. Internat. Verein. Limnol.* **24**: 963-967.

Siegenthaler C, Sturm M. 1991. Die Häufigkeit von Ablagerungen extremer Reuss-Hochwasser : Die Sedimentationsgeschichte im Urnersee seit dem Mittelalter. *Mitteilungen Bundesamt für Wasserwirtschaft* **4**: 127-139.

Simonneau A, Chapron E, Vannière B, Wirth SB, Gilli A, Di Giovanni C, Anselmetti FS, Desmet M, Magny M. 2013. Mass-movement and flood-induced deposits in Lake Ledro, southern Alps, Italy: implications for Holocene palaeohydrology and natural hazards. *Clim. Past* **9**: 825-840.

Sturm M, Matter A. 1978. Turbidites and varves in Lake Brienz (Switzerland): deposition of clastic detritus by density currents. *Spec. Publs int. Sediment.* **2**: 147-178.

Swierczynski T, Brauer A, Lauterbach S, Martín-Puertas C, Dulski P, von Grafenstein U, Rohr C. 2012. A 1600 yr seasonally resolved record of decadal-scale flood variability from the Austrian Pre-Alps. *Geology* **40**: 1047-1050.

Swierczynski T, Lauterbach S, Dulski P, Brauer A. 2009. Die Sedimentablagerungen des Mondsees (Oberösterreich) als ein Archiv extremer Abflussereignisse der letzten 100 Jahre, In: *Klimawandel in Österreich - Die letzten 20.000 Jahre...und ein Blick voraus*, Schmidt R, Matulla C, Psenner R (eds.). Innsbruck University Press: Innsbruck; 115-126.

Swierczynski T, Lauterbach S, Dulski P, Delgado J, Merz B, Brauer A. 2013. Mid- to late Holocene flood frequency changes in the northeastern Alps as recorded in varved sediments of Lake Mondsee (Upper Austria). *Quaternary Science Reviews* **80**: 78-90.

van Husen D, 1989. Blatt 65–Mondsee, Geologische Karte der Republik Österreich 1:50 000. Geologische Bundesanstalt, Wien.

Wilhelm B, Arnaud F, Sabatier P, Magand O, Chapron E, Courp T, Tachikawa K, Fanget B, Malet E, Pignol C, Bard E, Delannoy JJ. 2013. Palaeoflood activity and climate change over the last 1400 years recorded by lake sediments in the north-west European Alps. *Journal of Quaternary Science* **28**: 189-199.

Wirth SB, Gilli A, Simonneau A, Ariztegui D, Vannière B, Glur L, Chapron E, Magny M, Anselmetti FS. 2013. A 2000 year long seasonal record of floods in the southern European Alps. *Geophys. Res. Lett.* **40**: 4025-4029.

Supporting information

STable 1. Data on surface sediment cores from Lake Mondsee including the onset (sediment depth and time) of varve formation at individual coring sites.

Core name	Sampling	Lon (E)	Lat (N)	Water depth [m]	Core length [cm]	Trans. I/II Depth [cm]	Onset of varves [varve yr AD]
MO/10/1	Oct 2010	13°22'47.28"	47°49'34.02"	48.0	133.0	26.5	1957
MO/10/2	Oct 2010	13°22'46.68"	47°49'21.48"	52.0	134.0	28.0	1953
MO/10/3	Oct 2010	13°23'01.38"	47°49'10.32"	55.0	158.0	28.0	1954
MO/10/4	Oct 2010	13°22'47.10"	47°49'09.66"	55.0	143.0	27.5	1953
MO/10/5	Oct 2010	13°22'31.86"	47°49'09.90"	47.0	149.5	37.0	1953
MO/10/6	Oct 2010	13°22'17.70"	47°49'12.12"	34.0	141.5	-	-
MO/10/7	Oct 2010	13°22'40.56"	47°49'00.18"	54.0	148.0	28.0	1953
MO/10/8	Oct 2010	13°22'48.96"	47°48'46.74"	54.0	143.5	22.0	1957
MO/10/9	Oct 2010	13°23'06.72"	47°48'36.36"	59.0	160.0	18.0	1957
MO/07/SC7	Mar 2007	13°23'33.78"	47°48'30.42"	65.0	72.0	19.7	< 1953
MO/07/SC4	Mar 2007	13°24'01.68"	47°48'22.74"	64.0	68.0	18.2	< 1953
MO/05/P3	Jun 2005	13°24'05.46"	47°48'24.72"	62.0	97.0	11.9	< 1953
MO/07/SC3	Mar 2007	13°23' 59.46"	47°48'10.02"	60.0	70.5	17.5	1957